THE IMPORTANCE OF ELECTRON CAPTURES IN CORE-COLLAPSE SUPERNOVAE*

K. Langanke, J.M. Sampaio

Institut for Fysik og Astronomi, Århus Universitet
DK-8000 Århus C, Denmark

and G. Martínez-Pinedo

Institut d'Estudis Espacials de Catalunya
E-08034 Barcelona, Spain
and
Institució Catalana de Recerca i Estudis Avançats
E-08010 Barcelona, Spain

(Received January 21, 2004)

Nuclear physics plays an essential role in the dynamics of a type II supernova (a collapsing star). Recent advances in nuclear many-body theory allow now to reliably calculate the stellar weak-interaction processes involving nuclei. The most important process is the electron capture on finite nuclei with mass numbers $A > 55$. It is found that the respective capture rates, derived from modern many-body models, differ noticeably from previous, more phenomenological estimates. This leads to significant changes in the stellar trajectory during the supernova explosion, as has been found in state-of-the-art supernova simulations.

PACS numbers: 26.50.+x, 23.40.–s, 97.60.Bw, 21.60.Cs

1. Electron captures in core-collapse supernovae — the general picture

Massive stars end their lives as type II supernovae, triggered by a collapse of their central iron core with a mass of more than $1M_{\odot}$. The general picture of a core-collapse supernova is probably well understood and has been confirmed by various observations from supernova 1987A. Reviews on

* Presented at the XXVIII Mazurian Lakes School of Physics, Krzyże, Poland, August 31–September 7, 2003.

core-collapse supernovae can be found in [1, 2]. Nevertheless, the most sophisticated supernova simulations [3–5] currently fail to explode indicating that improved input or numerical treatment is required. Among these inputs are several nuclear ingredients (equation of state, nuclear processes mediated by the weak interaction, but also the $^{12}\mathrm{C}(\alpha,\gamma)^{16}\mathrm{O}$ reaction rate which influences the size of the final iron core). Recent progress in describing nuclear weak-interaction processes, made possible by improved many-body models and better computational facilities, is summarized in [6]. Here we focus on the electron capture on nuclei. Using advances in nuclear shell model developments, the relevant stellar rates have been calculated very recently. When employed in collapse simulations these rates lead to significant revisions clearly demonstrating the need for state-of-the-art nuclear physics models in nuclear astrophysics.

Late-stage stellar evolution is described in two steps. In the presupernova models the evolution is studied through the various hydrostatic core and shell burning phases until the central core density reaches values up to 10^{10} g/cm^3. The models consider a large nuclear reaction network. However, the densities involved are small enough to treat neutrinos solely as an energy loss source. For even higher densities this is no longer true as neutrino-matter interactions become increasingly important. In modern core-collapse codes neutrino transport is described self-consistently by spherically symmetric multigroup Boltzmann simulations [3–5]. While this is computationally very challenging, collapse models have the advantage that the matter composition can be derived from Nuclear Statistical Equilibrium (NSE) as the core temperature and density are high enough to keep reactions mediated by the strong and electromagnetic interactions in equilibrium. This means that for sufficiently low entropies, the matter composition is dominated by the nuclei with the highest Q-values for a given Y_e. The presupernova models are the input for the collapse simulations which follow the evolution through trapping, bounce and hopefully explosion.

The collapse is a competition of the two weakest forces in nature: gravity versus weak interaction, where electron captures on nuclei and protons and, during a period of silicon burning, also β-decay play the crucial roles. Which nuclei are important? Weak-interaction processes become important when nuclei with masses $A \sim 55$–60 (pf shell nuclei) are most abundant in the core (although capture on sd shell nuclei has to be considered as well). As weak interactions changes Y_e and electron capture dominates, the Y_e value is successively reduced from its initial value ~ 0.5. As a consequence, the abundant nuclei become more neutron-rich and heavier, as nuclei with decreasing Z/A ratios are more bound in heavier nuclei. Two further general remarks are useful. There are many nuclei with appreciable abundances in the cores of massive stars during their final evolution. Neither the nucleus with the largest capture rate nor the most abundant one are necessarily the most relevant for the dynamical evolution: What makes a nucleus relevant is the product of rate times abundance.

For densities $\rho < 10^{11}$ g/cm^3, stellar weak-interaction processes are dominated by Gamow–Teller (GT) and, if applicable, by Fermi transitions. At higher densities forbidden transitions have to be included as well. To understand the requirements for the nuclear models to describe these processes (mainly electron capture), it is quite useful to recognize that electron capture is governed by two energy scales: the electron chemical potential μ_e, which grows like $\rho^{1/3}$, and the nuclear Q-value. Further, μ_e grows much faster than the Q values of the abundant nuclei. We can conclude that at low densities, where one has $\mu_e \sim Q$ (*i.e.* at presupernova conditions), the capture rates will be very sensitive to the phase space and require an accurate as possible description of the detailed GT_+ distribution of the nuclei involved. Furthermore, the finite temperature in the star requires the implicit consideration of capture on excited nuclear states, for which the GT distribution can be different than for the ground state. As we will demonstrate below, modern shell model calculations are capable to describe GT_+ distributions rather well and are therefore the appropriate tool to calculate the weak-interaction rates for those nuclei ($A \sim$ 50–65) which are relevant at such densities. At higher densities, when μ_e is sufficiently larger than the respective nuclear Q values, the capture rate becomes less sensitive to the detailed GT_+ distribution and is mainly only dependent on the total GT strength. Thus, less sophisticated nuclear models might be sufficient. However, one is facing a nuclear structure problem which has been overcome only very recently. We come back to it below, after we have discussed the calculations of weak-interaction rates within the shell model and their implications to presupernova models.

2. Weak-interaction rates and presupernova evolution

The general formalism to calculate weak interaction rates for stellar environment has been given by Fuller, Fowler and Newman (FFN) [7–10]. These authors also estimated the stellar electron capture and beta-decay rates systematically for nuclei in the mass range $A =$ 20–60 based on the independent particle model and on data, whenever available. In recent years this pioneering and seminal work has been replaced by rates based on large-scale shell model calculations. At first, Oda *et al.* derived such rates for *sd*-shell nuclei (A = 17–39) and found rather good agreement with the FFN rates [11]. Similar calculations for *pf* shell nuclei had to wait until significant progress in shell model diagonalization, mainly due to Etienne Caurier, allowed calculations in either the full *pf* shell or at such a truncation level that the

GT distributions were virtually converged. It has been demonstrated in [12] that the shell model reproduces all measured GT_+ distributions very well and gives a very reasonable account of the experimentally known GT_- distributions. Further, the lifetimes of the nuclei and the spectroscopy at low energies is simultaneously also described well. Charge-exchange measurements using the (d,^{2}He) reaction at intermediate energies allow now for an experimental determination of the GT_+ strength distribution with an energy resolution of about 150 keV. Experimental GT_+ strengths, measured for several pf shell nuclei at the KVI in Groningen [15], agree well with shell model predictions. An example is shown in Fig. 1. It can be concluded that modern shell model approaches have the necessary predictive power to reliably estimate stellar weak interaction rates. Such rates have been presented in [13, 16] for more than 100 nuclei in the mass range $A = 45$–65. The rates have been calculated for the same temperature and density grid as the standard FFN compilations [8, 9]. An electronic table of the rates is available [16]. Importantly one finds that the shell model electron capture rates are systematically smaller than the FFN rates.

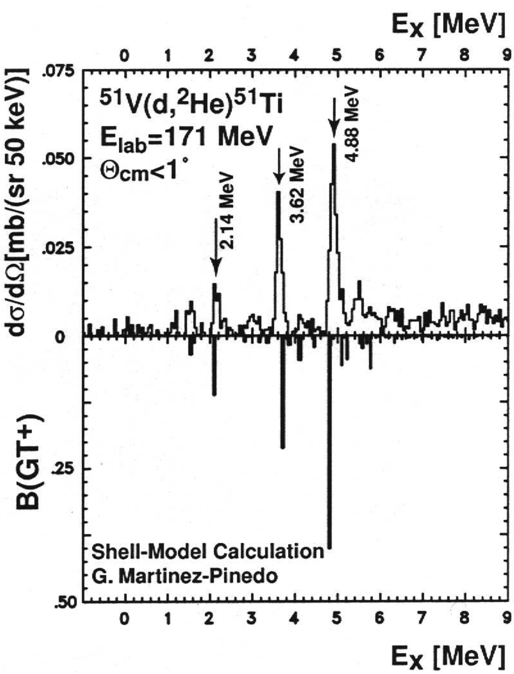

Fig. 1. Comparison of the measured ^{51}V(d,^{2}He)^{51}Ti cross section at forward angles (which is proportional to the GT_+ strength) with the shell model GT distribution in ^{51}V (from [14]).

To study the influence of the shell model rates on presupernova models Heger *et al.* [17,18] have repeated the calculations of Weaver and Woosley [19] keeping the stellar physics, except for the weak rates, as close to the original studies as possible. Fig. 2 exemplifies the consequences of the shell model weak interaction rates for presupernova models in terms of the three decisive quantities: the central Y_e value and entropy and the iron core mass. The central values of Y_e at the onset of core collapse increased by 0.01–0.015 for the new rates. This is a significant effect. We note that the new models also result in lower core entropies for stars with $M \leq 20M_\odot$, while for $M \geq 20M_\odot$, the new models actually have a slightly larger entropy. The iron core masses are generally smaller in the new models where the effect is larger for more massive stars ($M \geq 20M_\odot$), while for the most common supernovae ($M \leq 20M_\odot$) the reduction is by about 0.05 $M_\odot$.

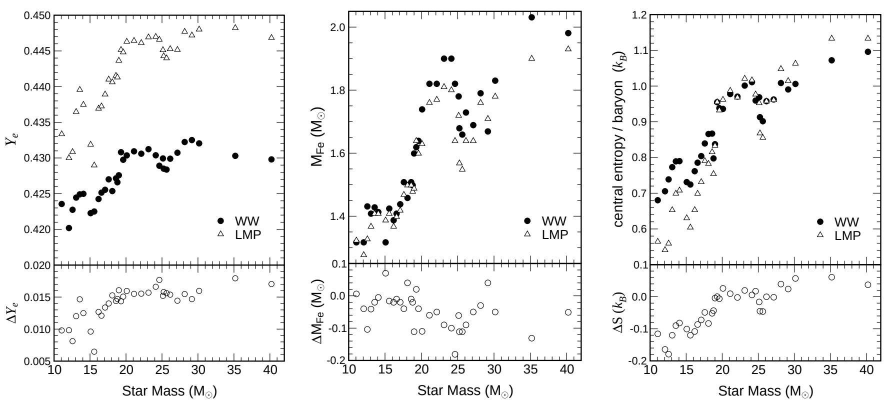

Fig. 2. Comparison of the center values of Y_e (left), the iron core sizes (middle) and the central entropy (right) for 11–40 $M_\odot$ stars between the WW models, which used the FFN rates, and the ones using the shell model weak interaction rates (LMP).

Electron capture dominates the weak-interaction processes during presupernova evolution. However, during silicon burning, β decay (which increases Y_e) can compete and adds to the further cooling of the star. With increasing densities, β-decays are hindered as the increasing Fermi energy of the electrons blocks the available phase space for the decay. Thus, during collapse β-decays can be neglected (see next section).

We note that the shell model weak interaction rates predict the presupernova evolution to proceed along a temperature-density-Y_e trajectory where the weak processes are dominated by nuclei rather close to stability. Thus it will be possible, after radioactive ion-beam facilities become operational, to further constrain the shell model calculations by measuring relevant beta decays and GT distributions for unstable nuclei. Ref. [17, 18] identify those nuclei which dominate (defined by the product of abundance times rate) the electron capture and beta decay during various stages of the final evolution of a $15M_\odot$, $25M_\odot$ and $40M_\odot$ star.

3. The role of electron capture during collapse

In collapse simulations a very simple description for electron capture on nuclei has been used until recently, as the rates have been estimated in the spirit of the independent particle model (IPM), assuming pure Gamow–Teller (GT) transitions and considering only single particle states for proton and neutron numbers between $N = 20$–40 [20]. In particular this model assigns vanishing electron capture rates to nuclei with neutron numbers larger than $N = 40$, motivated by the observation [21] that, within the IPM, GT transitions are Pauli-blocked for nuclei with $N \geq 40$ and $Z \leq 40$. However, as electron capture reduces Y_e, the nuclear composition is shifted to more neutron rich and to heavier nuclei, including those with $N > 40$, which dominate the matter composition for densities larger than a few 10^{10} g cm^{-3}. As a consequence of the model applied in the previous collapse simulations, electron capture on nuclei ceases at these densities and the capture is entirely due to free protons. This employed model for electron capture on nuclei is too simple and leads to incorrect conclusions, as the Pauli-blocking of the GT transitions is overcome by correlations [22] and temperature effects [21, 23].

At first, the residual nuclear interaction, beyond the IPM, mixes the pf shell with the levels of the sdg shell, in particular with the lowest orbital, $g_{9/2}$. This makes the closed $g_{9/2}$ orbit a magic number in stable nuclei ($N = 50$) and introduces, for example, a very strong deformation in the $N = Z = 40$ nucleus ^{80}Zr [24]. Moreover, the description of the B(E2,$0^+ \to 2_1^+$) transition in ^{68}Ni requires configurations where more than one neutron is promoted from the pf shell into the $g_{9/2}$ orbit [25], unblocking the GT transition even in this proton-magic $N = 40$ nucleus. Such a non-vanishing GT strength has already been observed for ^{72}Ge ($N = 40$) [26] and ^{76}Se ($N = 42$) [27]. Secondly, during core collapse electron capture on the nuclei of interest here occurs at temperatures $T > 0.8$ MeV, which, in the Fermi gas model, corresponds to a nuclear excitation energy $U \approx AT^2/8 > 5$ MeV; this energy is noticeably larger than the splitting of the pf and sdg orbitals ($E_{g_{9/2}} - E_{p_{1/2},f_{5/2}} \approx 3$ MeV). Hence, the configuration mixing of sdg and pf orbitals will be rather strong in those excited nuclear states of relevance for stellar electron capture. Furthermore, the nuclear state density at $E \sim 5$ MeV is already larger than 100/MeV, making a state-by-state calculation of the rates impossible, but also emphasizing the need for a nuclear model which describes the correlation energy scale at the relevant temperatures appropriately. This model is the Shell Model Monte Carlo (SMMC) approach [28, 29] which describes the nucleus by a canonical ensemble at finite temperature and employs a Hubbard-Stratonovich linearization [30] of the imaginary-time many-body propagator to express observables as path integrals of one-body propagators in fluctuating auxiliary fields [28, 29]. Since Monte Carlo techniques avoid an explicit enumeration of the many-body states, they can be used in model spaces far larger than those accessible to conventional methods. The Monte Carlo results are in principle exact and are in practice subject only to controllable sampling and discretization errors.

To calculate electron capture rates for nuclei $A = 65$–112 SMMC calculations have been performed in the full pf–sdg shell [31], using a residual pairing+quadrupole interaction, which, in this model space, reproduces well the collectivity around the $N = Z = 40$ region and the observed low-lying spectra in nuclei like ^{64}Ni and ^{64}Ge. From the SMMC calculations the temperature-dependent occupation numbers of the various single-particle orbitals have been determined. These occupation numbers then became the input in RPA calculations of the capture rate, considering allowed and forbidden transitions up to multipoles $J = 4$ and including the momentum dependence of the operators. The method has been validated against capture rates calculated from diagonalization shell model studies for ^{64,66}Ni. The model is described in [22]; first applications in collapse simulations are presented in [33, 34].

Simulations of core collapse require reaction rates for electron capture on protons, $R_p = Y_p\lambda_p$, and nuclei $R_h = \sum_i Y_i\lambda_i$ (where the sum runs over all the nuclei present and Y_i denotes the number abundance of a given species), over wide ranges in density and temperature. While R_p is readily derived from [20], the calculation of R_h requires knowledge of the nuclear composition, in addition to the electron capture rates described earlier. In [33, 34] a Saha-like NSE has been adopted to determine the needed abundances of individual isotopes and to calculate R_h and the associated emitted neutrino spectra on the basis of about 200 nuclei in the mass range $A = 45$–112 as a function of temperature, density and electron fraction. The rates for the inverse neutrino-absorption process are determined from the electron capture rates by detailed balance. Due to its much smaller $|Q|$-value, the electron capture rate on the free protons is larger than the rates of abundant nuclei during the core collapse. However, this is misleading as the low entropy keeps the protons significantly less abundant than heavy nuclei during the collapse. Fig. 3 shows that the reaction rate on nuclei, R_h, dominates the one on protons, R_p, by roughly an order of magnitude throughout the collapse when the composition is considered. (We note that this figure is based on a stellar trajectory which does not consider capture on nuclei. We will see below that this process dominates and reduces Y_e even more. As a consequence the abundance of free protons in NSE is significantly reduced, making capture on free protons even less important.) Only after the bounce shock has formed does R_p become higher than R_h, due to the high entropies and high temperatures in the shock-heated matter that result in a high proton abundance. The obvious conclusion is that electron capture on nuclei must be included in collapse simulations.

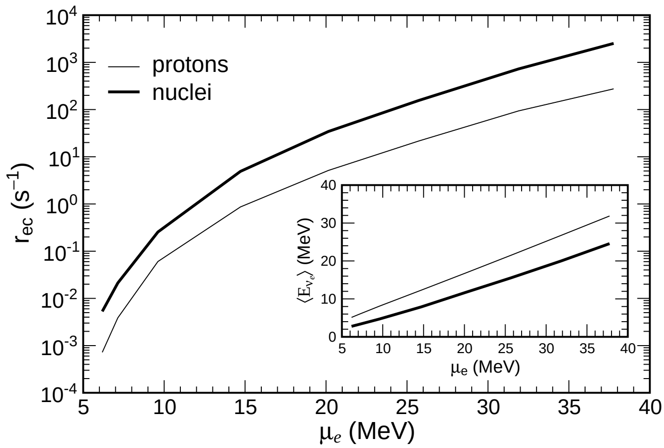

Fig. 3. The reaction rates for electron capture on protons (thin line) and nuclei (thick line) are compared as a function of electron chemical potential along a stellar collapse trajectory. The insert shows the related average energy of the neutrinos emitted by capture on nuclei and protons. The results for nuclei are averaged over the full nuclear composition (see text). Neutrino blocking of the phase space is not included in the calculation of the rates.

It is also important to stress that electron capture on nuclei and on free protons differ quite noticeably in the neutrino spectra they generate. This is demonstrated in Fig. 3 which shows that neutrinos from captures on nuclei have a mean energy 40–60% less than those produced by capture on protons. Although capture on nuclei under stellar conditions involves excited states in the parent and daughter nuclei, it is mainly the larger $|Q|$-value which significantly shifts the energies of the emitted neutrinos to smaller values. These differences in the neutrino spectra strongly influence neutrino-matter interactions, which scale with the square of the neutrino energy and are essential for collapse simulations [4, 5].

The effects of this more realistic implementation of electron capture on heavy nuclei have been evaluated in independent self-consistent neutrino radiation hydrodynamics simulations by the Oak Ridge and Garching collaborations [34, 35]. The basis of these models is described in detail in Refs. [5] and [4]. Both collapse simulations yield qualitatively the same results. The changes compared to the previous simulations, which adopted the IPM rate estimate from Ref. [20] and hence basically ignored electron capture on nuclei, are significant. Fig. 4 shows a key result: In denser regions, the additional electron capture on heavy nuclei results in more electron capture in the new models. In lower density regions, where nuclei with $A < 65$ domi-

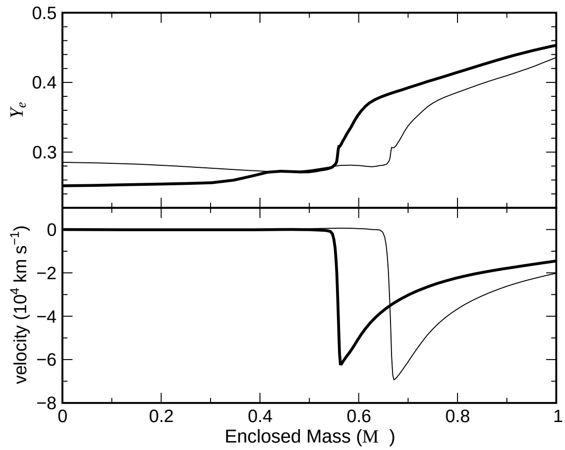

Fig. 4. The electron fraction and velocity as functions of the enclosed mass at bounce for a 15 $M_\odot$ model [17]. The thin line is a simulation using the Bruenn parameterization while the thick line is for a simulation using the combined LMP [13] and SMMC+RPA rate sets.

nate, the shell model rates [13] result in less electron capture. The results of these competing effects can be seen in the first panel of figure 4, which shows the distribution of Y_e throughout the core at bounce (when the maximum central density is reached). The combination of increased electron capture in the interior with reduced electron capture in the outer regions causes the shock to form with 16% less mass interior to it and a 10% smaller velocity difference across the shock. This leads to a smaller mass of the homologous core (by about 0.1 $M_\odot$). In spite of this mass reduction, the radius from which the shock is launched is actually displaced slightly outwards to 15.7 km from 14.8 km in the old models. If the only effect of the improvement in the treatment of electron capture on nuclei were to launch a weaker shock with more of the iron core overlying it, this improvement would seem to make a successful explosion more difficult. However, the altered gradients in density and lepton fraction also play an important role in the behavior of the shock. Though also the new models fail to produce explosions in the spherically symmetric limit, the altered gradients allow the shock in the case with improved capture rates to reach 205 km, which is about 10 km further out than in the old models.

These calculations clearly show that the many neutron-rich nuclei which dominate the nuclear composition throughout the collapse of a massive star also dominate the rate of electron capture. Astrophysics simulations have demonstrated that these rates have a strong impact on the core collapse trajectory and the properties of the core at bounce. The evaluation of the rates has to rely on theory as a direct experimental determination of the rates for the relevant stellar conditions (*i.e.* rather high temperatures) is currently impossible. Nevertheless it is important to experimentally explore the configuration mixing between pf and sdg shell in extremely neutron-rich nuclei as such understanding will guide and severely constrain nuclear models. Such guidance is expected from future radioactive ion-beam facilities.

4. Conclusions

The recent advances in nuclear many-body modelling has led to noticeable improvements in the nuclear input for core-collapse supernova models. It has been proven that the dynamical timescale of the final collapse is dominated by electron capture on nuclei, and not, as has been the standard picture for many years, by capture on free protons. This has significant consequences for the collapse and changes the Y_e and density profiles throughout the core. However, first supernova simulations do not yield successful explosions. In the meantime, several minor improvements with respect to the incorporation of electron capture in collapse simulations have been derived. These include a consistent treatment of plasma screening corrections which reduce the rates, but apparently lead to no significant changes in the simulations. Further, detailed neutrino spectra have been derived for the capture on individual nuclei (and their NSE average) as function of temperature, density and Y_e values. Possible consequences are expected to be small, but need to be explored.

For the future, other nuclear input needs improvements as well. At first, inelastic neutrino scattering on nuclei should be included in the simulations. The relevant cross sections can be calculated on the basis of the nuclear shell model (for allowed transitions) and the Random Phase Approximation (for forbidden transitions). A campaign calculating inelastic cross sections (as function of initial and final neutrino energies and at finite temperatures) for about 60 nuclei in the relevant $A \sim 60$ mass range is finished and the rates are currently incorportated into the codes. In another important step it is possible for non-deformed nuclei, like ^{52}Cr or ^{50}Ti, to constrain the dominating allowed contributions to the inelastic cross sections from precision (e, e') data showing quite remarkable agreement with the shell model predictions.

The Equation of State plays also an essential role during the collapse, in particular the symmetry energy component and the compression modulus at finite temperatures. Neutrino transport in dense matter requires the consideration of nucleon–nucleon correlations. First attempts into this direction have been taken based on RPA calculations, but more sophisticated approaches are desirable. Besides better nuclear input, improved description of multidimensional effects in supernova models will attract much attention in coming years. This will also include the effects of rotation or magnetic fields on the explosions.

The work presented here has benefitted from fruitful discussions and collaborations with David Dean, Alexander Heger, Raphael Hix, Thomas Janka, Tony Mezzacappa, Bronson Messer, Matthias Liebendörfer and Stan Woosley. The work has been partly supported by the Danish Research Council and by the Spanish MCYT. JMS acknowledges the financial support of the Portuguese "Fundação para a Ciência e Tecnologia".

REFERENCES

[1] H.A. Bethe, *Rev. Mod. Phys.* **62**, 801 (1990).

[2] H.-Th. Janka, K. Kifonidis, M. Rampp, *Lect. Notes Phys.* **578**, 333 (2001).

[3] R. Buras, M. Rampp, H.-Th. Janka, K. Kifonidis, *Phys. Rev. Lett.* **90**, 241101 (2003).

[4] H.Th. Janka, M. Rampp, *Astrophys. J.* **539**, L33 (2000).

[5] A. Mezzacappa *et al.*, *Phys. Rev. Lett.* **86**, 1935 (2001).

[6] K. Langanke, G. Martinez-Pinedo, *Rev. Mod. Phys.* **75**, 819 (2003).

[7] G.M. Fuller, W.A. Fowler, M.J. Newman, *ApJS* **42**, 447 (1980).

[8] G.M. Fuller, W.A. Fowler, M.J. Newman, *ApJS* **48**, 279 (1982).

[9] G.M. Fuller, W.A. Fowler, M.J. Newman, *ApJ* **252**, 715 (1982).

[10] G.M. Fuller, W.A. Fowler, M.J. Newman, *ApJ* **293**, 1 (1985).

[11] T. Oda, M. Hino, K. Muto, M. Takahara, K. Sato, *At. Data Nucl. Data Tables* **56**, 231 (1994).

[12] E. Caurier, K. Langanke, G. Martínez-Pinedo, F. Nowacki, *Nucl. Phys.* **A653**, 439 (1999).

[13] K. Langanke, G. Martínez-Pinedo, *Nucl. Phys.* **A673**, 481 (2000).

[14] C. Bäumer *et al.*, *Phys. Rev.* **C**, in print.

[15] D. Frekers, Proccedings COMEX1, *Nucl. Phys.* **A**, to be published.

[16] K. Langanke, G. Martínez-Pinedo, *At. Data Nucl. Data Tables* **79**, 1 (2001).

[17] A. Heger, K. Langanke, G. Martinez-Pinedo, S.E. Woosley, *Phys. Rev. Lett.* **86**, 1678 (2001).

[18] A. Heger, S.E. Woosley, G. Martinez-Pinedo, K. Langanke, *Astr. J.* **560**, 307 (2001).

[19] S.E. Woosley, T.A. Weaver, *Astrophys. J. Suppl.* **101**, 181 (1995).

[20] S.W. Bruenn, *Astrophys. J. Suppl.* **58**, 771 (1985); A. Mezzacappa, S.W. Bruenn, *Astrophys. J.* **405**, 637 (1993); **410**, 740 (1993).

[21] G.M. Fuller, *Astrophys. J.* **252**, 741 (1982).

[22] K. Langanke, E. Kolbe, D.J. Dean, *Phys. Rev.* **C63**, 032801 (2001).

[23] J. Cooperstein, J. Wambach, *Nucl. Phys.* **A420**, 591 (1984).

[24] W. Nazarewicz, J. Dudek, R. Bengtsson, T. Bengtsson, I. Ragnarsson, *Nucl. Phys.* **A435**, 397 (1985).

[25] O. Sorlin *et al.*, *Phys. Rev. Lett.* **88**, 092501 (2002).

[26] M.C. Vetterli *et al.*, *Phys. Rev.* **C45**, 997 (1992).

[27] R.L. Helmer *et al.*, *Phys. Rev.* **C55**, 2802 (1997).

[28] C.W. Johnson, S.E. Koonin, G.H. Lang, W.E. Ormand, *Phys. Rev. Lett.* **69**, 3157 (1992).

[29] S.E. Koonin, D.J. Dean, K. Langanke, *Phys. Rep.* **278**, 2 (1997).

[30] J. Hubbard, *Phys. Lett.* **3**, 77 (1959); R.D. Stratonovich, *Sov. Phys.-Dokl.* **2**, 416 (1958).

[31] J.M. Sampaio, Ph.D. thesis, University of Aarhus, 2003.

[32] W.R. Hix, Ph.D. thesis, Harvard University, 1995.

[33] K. Langanke *et al.*, *Phys. Rev. Lett.* **90**, 241102 (2003).

[34] R.W. Hix *et al.*, *Phys. Rev. Lett.*, **91**, 201102 (2003).

[35] H-Th. Janka *et al.*, to be published.